

Higher-order Kerr improve quantitative modeling of laser filamentation

M. Petrarca¹, Y. Petit¹, S. Henin¹, R. Delagrangé¹, P. Béjot^{1,2}, J. Kasparian^{1,*}

(1) *GAP-Biophotonics, Université de Genève, Chemin de Pinchat 22, 1211 Geneva 4, Switzerland*

(2) *Laboratoire Interdisciplinaire Carnot de Bourgogne (ICB), UMR 5209 CNRS-Université de Bourgogne, BP 47870, F-21078 Dijon Cedex, France*

* *jerome.kasparian@unige.ch*

We test numerical filamentation models against experimental data about the peak intensity and filament density in laser filaments. We show that the consideration of the higher-order Kerr effect (HOKE) improves the quantitative agreement without the need of adjustable parameters. © 2012 Optical Society of America

OCIS codes: 320.2250, 190.3270, 320.7110, 190.5940

Laser filamentation [1–4] is a propagation regime typical of high-power lasers. It stems from a dynamic balance between self-focusing and self-defocusing non-linearities of different orders, i.e., different intensity dependences. Self-focusing by the Kerr effect is well established. Conversely, the relative contributions to defocusing are still discussed. The two main effects nowadays considered in gases are the laser-generated plasma and the saturation of the medium polarisability under strong-field illumination [5–7], empirically described as a power series of the intensity and referred to as higher-order Kerr effect (HOKE). The latter have been first introduced as freely adjustable parameters [8,9], before experimental values were reported [10,11].

Strong effort have been dedicated to reach a quantitative agreement between numerical models of non-linear pulse propagation and experimental data about filamentation [12–15]. In that purpose, a common approach consists in tweaking simulation inputs like the non-linear index or the ionization rates, and/or the experimental parameters such as the beam energy, pulse duration, beam diameter or profile, until a satisfactory match with the experiments is achieved. The remaining discrepancies are generally attributed, among others, to the difficulty of the experimental measurements inside the filaments, and the associated

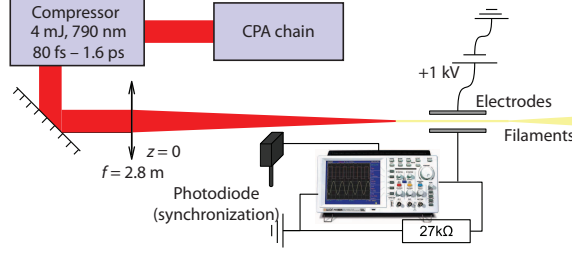


Fig. 1. Experimental setup

uncertainties. However, the introduction of new techniques, e.g. for measuring the peak intensity from the ratio of nitrogen fluorescence lines [16,17] enhances the precision and renew the challenge for theoretical models to precisely match those data.

Here, we provide experimental electron density measurements over a wide range of pulse durations, and compare these experimental results with numerical simulations. We show that considering the HOKE in the model allows a good agreement between experimental results and simulations without any parameter adjustment. Such agreement is also confirmed when comparing the model including the HOKE [18] with previously published data about the filament peak intensity [17] and electron density [19].

The filament ionization was characterized as a function of the pulse duration by using 4 mJ laser pulses centered at 800 nm, with 100 Hz repetition rate and 3 cm initial beam diameter. The slightly diverging beam was focused by an $f=2.8$ m lens to form a 20 cm long filament in air. The pulse duration was varied from 80 fs to 1.6 ps by detuning the grating compressor of the chirped pulse amplification (CPA) chain. The charge is measured by propagating the filaments between a pair of parallel electrodes (1 x 1 cm; 1 cm spacing) under 1 kV bias: the transient current through the circuit is proportional to the electron density generated by the filaments [20], although with an arbitrary calibration factor (See Figure 1). This charge measurement was double-checked by sonometric measurements [21].

To get information about the role of the HOKE, we performed numerical simulations considering a linearly polarized incident electric field at a wavelength $\lambda_0=800$ nm with cylindrical symmetry around the propagation axis z . According to the unidirectional propagation pulse equation (UPPE) [22], the scalar envelope $\varepsilon(r, t, z)$ (defined such that $|\varepsilon(r, z, t)|^2 = I(r, z, t)$, I being the intensity) evolves in the frame traveling at the pulse velocity according to [23]:

$$\begin{aligned} \partial_z \tilde{\varepsilon} = & i(\sqrt{k^2(\omega) - k_{\perp}^2} - k' \omega) \tilde{\varepsilon} \\ & + \frac{1}{\sqrt{k^2(\omega) - k_{\perp}^2}} \left(\frac{i\omega^2}{c^2} \tilde{P}_{\text{NL}} - \frac{\omega}{2\epsilon_0 c^2} \tilde{J} \right) - \tilde{\alpha}, \end{aligned} \quad (1)$$

where c is the velocity of light in vacuum, ω is the angular frequency, $k(\omega)=n(\omega)\omega/c$, k' its

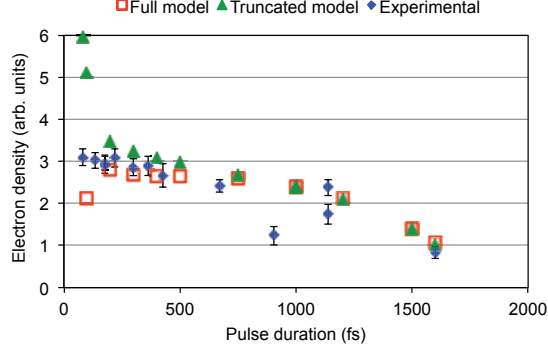


Fig. 2. Effect of pulse duration on the electron density in filaments. Each numerical curve is normalized independently to optimally match the experimental results.

derivative at $\omega_0 = 2\pi c/\lambda_0$, $n(\omega)$ is the linear refractive index at the frequency ω , k_\perp is the spatial angular frequency. P_{NL} is the nonlinear polarization, J is the free-charge induced current and α is the nonlinear losses induced by photo-ionization. \tilde{f} denotes simultaneous temporal Fourier and spatial Hankel transforms of function f . The non-linear polarization is evaluated as $P_{\text{NL}} = \left(\sum_j n_{2j} |\varepsilon|^{2j} + \Delta n_{\text{Raman}} \right) \varepsilon$, where the n_{2j} are the j^{th} -order nonlinear refractive indices ($n_2 = 1.2 \times 10^{-7} \text{ cm}^2/\text{TW}$, $n_4 = -1.5 \times 10^{-9} \text{ cm}^4/\text{TW}^2$, $n_6 = 2.1 \times 10^{-10} \text{ cm}^6/\text{TW}^3$, $n_8 = -8 \times 10^{-12} \text{ cm}^8/\text{TW}^4$ [10]) and Δn_{Raman} is the Raman induced refractive index change evaluated by solving the rotational time-dependent Schrödinger equation of both N_2 and O_2 in the weak field regime. Alternatively, the model is truncated to the third-order non-linearity (i.e. the $n_2 |\varepsilon|^2 \varepsilon$ term) to disregard the contribution of the HOKE. The current is evaluated as $\tilde{J} = \frac{e^2}{m_e} (\nu_e + i\omega) \tilde{\rho} \varepsilon / (\nu_e^2 + \omega^2)$, where e and m_e are the electron charge and mass respectively, ϵ_0 is the vacuum permittivity, ν_e is the effective electronic collisional frequency, and ρ is the electron density. Finally, $\alpha = \sum_{i=\text{O}_2, \text{N}_2} W_i(|\varepsilon|^2) U_i \rho_{\text{at},i} / (2|\varepsilon|^2)$, $\rho_{\text{at},i}$ is the density of molecules of species i , $W_i(|\varepsilon|^2)$ is their photoionization probability modeled by the PPT formulation, with ionization potential U_i .

The propagation dynamics of the electric field is coupled with the electron density ρ , calculated as [2]

$$\partial_t \rho = \sum_{i=\text{O}_2, \text{N}_2} \left(W_i(|\varepsilon|^2) \rho_{\text{at},i} + \frac{\sigma_i}{U_i} \rho |\varepsilon|^2 \right) - \beta \rho^2, \quad (2)$$

where β are the electron recombination rate and σ_i are the inverse Bremsstrahlung cross-sections with species i , also accounting for avalanche ionization. Note that our model relies only on published values [4, 10] and contains no adjustable parameter. For each experimental situation, we directly used the experimental parameters, without any tweaking. Unless otherwise specified, Gaussian pulse shapes have been considered, both spatially and temporally.

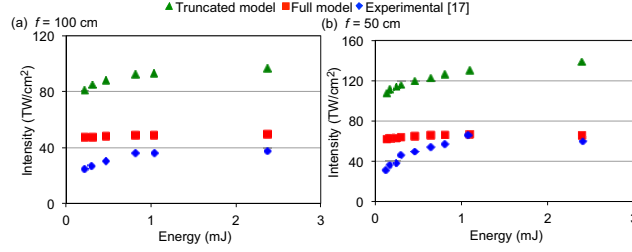


Fig. 3. Experimental [17] and simulated peak intensity in filaments generated by 42 fs pulses of 1 cm diameter, focused with (a) $f = 1$ cm and (b) $f=50$ cm.

The measured electron density rose very slowly (less than a factor of 4) when the pulse duration was decreased from 1.6 ps to 80 fs, although the peak power drastically increased by a factor of 20 (Figure 2). This might seem unexpected when considering that the ionization rate scales with I^8 in oxygen [24, 25]. This relative stability can however be understood by considering that the free electrons need several picoseconds to tens of ps to recombine, so that they accumulate more efficiently during longer pulses, an effect that partly balances the lower ionization rates. While both models reproduce this slow variation for pulses below a few hundreds of femtoseconds, the full model seems slightly more accurate for shorter pulses.

To get a more direct comparison between the two models, we successively tested them against previously published *quantitative* experimental data about the peak intensity [17] and electron density [19] measured in filaments by different groups and techniques, so as to avoid individual artifacts or systematic errors to affect our conclusions.

As shown in Figure 3, the peak intensity of filaments generated by focused 42 fs pulses of 1 cm diameter at $1/e^2$ (i.e, 5.9 mm FWHM) measured via the ratio of nitrogen fluorescence lines [17] is much better reproduced by the full model than by the truncated one. The latter, in which the HOKE defocusing terms are disregarded, overestimates the intensity by a factor of typically 2–3.

The electron density as measured in [19] provides a much more sensitive variable, because its high-order dependence on intensity magnifies the experiment dynamics, allowing more reliable comparisons. The intensity of the nitrogen fluorescence constitutes a classical measurement of the electron density [26]. Consistent with the differences in the predicted intensities, the full model always yields a 4- to 30-times lower electron density than the truncated one. The match with experimental data [19] is perfect for a parallel beam corresponding to typical filamentation conditions (Figure 4a). However (Figure 4b–d), even the full model tends to overestimate the electron density produced by focused beams. This discrepancy could be due to the recently suggested overestimation [7] of the free electron density by the PPT model [4, 24], or to optical aberrations and astigmatism in experiments,

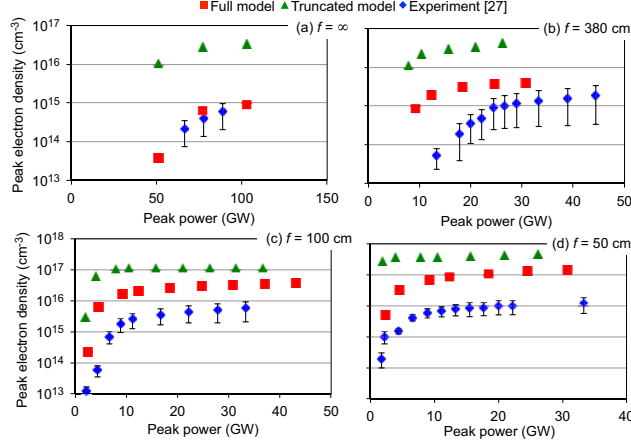


Fig. 4. Experimental [19] and simulated electron density as a function of focusing and incident power, for a 45 fs pulse of initial beam diameter of 8.4 mm (full width at $1/e^2$), for (a) a free-propagating (parallel) beam; (b) $f = 380$ cm; (c) $f = 100$ cm; (d) $f = 50$ cm.

which are not included in the model and tend to decrease the peak intensity in the waist region [27] and reduce filament length and strength [28]. Besides, this increasing geometrical constraint explains the decrease of the difference between the two models for tighter focusing. Therefore, the most concluding conditions to test filamentation models correspond the less focused ones, i.e. the larger f number.

Our results show that considering the saturation of the medium polarization in the strong-field regime (aka HOKE) improves the quantitative modeling of filamentation, especially for collimated beams for which the geometrical constraint does not interfere with the self-guiding process. Such update of the standard laser filamentation model is easy to implement, based on both experimental measurement [10] and quantum mechanical justifications [5–7]. It will in particular impact the determination of the optimal conditions for the potential atmospheric applications [29, 30] of laser filamentation, like rainmaking [31], or lightning control [32].

Acknowledgments. This work was supported by the European Research Council Advanced Grant "Filatmo" and the Conseil Régional de Bourgogne (FABER program). We thank F. Théberge for their assistance in accessing their experimental data reproduced in Figure 4 [19].

References

1. A. Braun, G. Korn, X. Liu, D. Du, J. Squier, G. Mourou. Self-channeling of high-peak-power femtosecond laser pulses in air, *Optics Letters*, **20**, 73 (1995)
2. A. Couairon and A. Mysyrowicz. Femtosecond filamentation in transparent media, *Phys. Rep.* **441**, 47 (2007).

3. S. L. Chin, S.A. Hosseini, W. Liu, Q. Luo, F. Théberge, N. Aközbek, A. Becker, V.P. Kandidov, O.G. Kosareva, and H. Schroeder. The propagation of powerful femtosecond laser pulses in optical media: physics, applications, and new challenges, *Can. J. Phys.* **83**, 863-905 (2005)
4. L. Bergé, S. Skupin, R. Nuter R, J. Kasparian, and J.-P. Wolf. Ultrashort filaments of light in weakly-ionized, optically-transparent media, *Rep. Prog. Phys.* **70**, 1633-1713 (2007).
5. E. A. Volkova, A. M. Popov, O. V. Tikhonova. Nonlinear Polarization Response of an Atomic Gas Medium in the Field of a High Intensity Femtosecond Laser Pulse, *JETP Letters* **94**, 519–524 (2011).
6. F. Morales, M. Richter, S. Patchkovskii, O. Smirnova, Imaging the Kramers-Henneberger atom, *Proceedings of the National Academy of Sciences* **187**, 16906-16911 (2011)
7. P. Bédot, E. Cormier, E. Hertz, B. Lavorel, J. Kasparian, J.-P. Wolf, and O. Faucher, On quantum mechanical origin of higher-order Kerr effect in gases: induced resonances and channel closure, submitted to *Phys. Rev. Lett.* arXiv:1206.4906v3 (2012)
8. D. L. Hovhannisyanyan. Analytic solution of the wave equation describing dispersion-free propagation of a femtosecond laser pulse in a medium with cubic and fifth-order nonlinearity, *Optics Communications*, **196**, 103 (2001)
9. A. Vinçotte, L. Bergé. $\chi^{(5)}$ susceptibility stabilizes the propagation of ultrashort laser pulses in air, *Physical Review A*, **70**, 061802(R) (2004)
10. V. Loriot, E. Hertz, O. Faucher, and B. Lavorel. Measurement of high order Kerr refractive index of major air components, *Opt. Express.* **17**, 13429 (2009); Erratum in *Opt. Express* **18** 3011 (2010)
11. V. Loriot, P. Bédot, W. Ettoumi, Y. Petit, J. Kasparian, S. Henin, E. Herz, B. Lavorel, O. Faucher, and J.-P. Wolf. On negative higher-order Kerr effect and filamentation, *Laser Physics*, **21**, 1319-1328 (2011)
12. S. Skupin, G. Stibenz, L. Bergé, F. Lederer, T. Sokollik, M. Schnurer, N. Zhavoronkov, G. Steinmeyer Self-compression by femtosecond pulse filamentation: Experiments versus numerical simulations, *Physical Review E*, **74**, 043813 (2006)
13. S. Champeaux, L. Berge, D. Gordon, A. Ting, J. Penano, P. Sprangle (3 + 1)-dimensional numerical simulations of femtosecond laser filaments in air: Toward a quantitative agreement with experiments, *Physical Review E (Statistical, Nonlinear, and Soft Matter Physics)*, **77**, 036406-6 (2008)
14. P. Polynkin, M. Kolesik, E. M. Wright, J. V. Moloney, Experimental Tests of the New Paradigm for Laser Filamentation in Gases, *Physical Review Letters*, **106**, 153902 (2011)
15. M. Kolesik, D. Mirell, J.-C. Diels, J. V. Moloney, On the higher-order Kerr effect in femtosecond filaments, *Optics Letters*, **35**, 3685-3687 (2010)

16. J.-F. Daigle, A. Jaron-Becker, S. Hosseini, T.-J. Wang, Y. Kamali, G. Roy, A. Becker, S. L. Chin Intensity clamping measurement of laser filaments in air at 400 and 800 nm, *Physical Review A*, **82**, 023405 (2010)
17. S. Xu, X. Sun, B. Zeng, W. Chu, J. Zhao, W. Liu, Y. Cheng, Z. Xu, S. L. Chin, Simple method of measuring laser peak intensity inside femtosecond laser filament in air, *Optics Express*, **20**, 299-307 (2012)
18. P. Béjot, J. Kasparian, S. Henin, V. Loriot, T. Vieillard, E. Hertz, O. Faucher, B. Lavorel, and J.-P. Wolf. Higher-order Kerr terms allow ionization-free filamentation in gases, *Phys. Rev. Lett.* **104**, 103903 (2010)
19. F. Théberge, W. W. Liu, P. T. Simard, A. Becker, S. L. Chin, Plasma density inside a femtosecond laser filament in air: Strong dependence on external focusing, *Physical Review E*, **74**, 036406 (2006)
20. S. Henin, Y. Petit, D. Kiselev, J. Kasparian, J.-P. Wolf. Contribution of water droplets to charge release by laser filaments in air, *Applied Physics Letters* **95**, 091107 (2009)
21. J. Yu, D. Mondelain, J. Kasparian, E. Salmon, S. Geffroy, C. Favre, V. Boutou, J. P. Wolf. Sonographic probing of laser filaments in air, *Applied Optics*, **42**, 7117 (2003)
22. M. Kolesik and J.V. Moloney. Nonlinear optical pulse propagation simulation: From Maxwell's to unidirectional equations, *Phys. Rev. E* **70**, 036604 (2004)
23. P. Béjot, E. Hertz, B. Lavorel, J. Kasparian, J.-P. Wolf, O. Faucher. Transition from plasma- to Kerr-driven laser filamentation, *Physical Review Letters* **106**, 243902 (2011)
24. A. Talebpour, J. Yang, S. L. Chin. Semi-empirical model for the rate of tunnel ionization of N₂ and O₂ molecule in an intense Ti:sapphire laser pulses, *Optics Communications*, **163**, 29-32 (1999)
25. J. Kasparian, R. Sauerbrey, and S.L. Chin. The critical laser intensity of self-guided light filaments in air, *Appl. Phys. B* **71**, 877-879 (2000)
26. S. A. Hosseini, J. Yu, Q. Luo, S. L. Chin. Multi-parameter characterization of the longitudinal plasma profile of a filament: a comparative study, *Applied Physics B*, **79**, 519 (2004)
27. Q. Sun, H.B. Jiang, Y. Liu, Y.H. Zhou, H. Yang, Q.H. Gong Effect of spherical aberration on the propagation of a tightly focused femtosecond laser pulse inside fused silica, *J. Opt. A: Pure Appl. Opt.* **7**, 655 (2005)
28. Y. Kamali, Q. Sun, J.-F. Daigle, A. Azarm, J. Bernhardt, S.L. Chin Lens tilting effect on filamentation and filament-induced fluorescence *Optics Communications* **282**, 950 (2008)
29. J. Kasparian, M. Rodriguez, G. Méjean, J. Yu, E. Salmon, H. Wille, R. Bourayou, S. Frey, Y.B. André, A. Mysyrowicz, R. Sauerbrey, J.-P. Wolf, and L. Wöste, *Science* **301**(5629), 61-64 (2003)
30. J. Kasparian and J.-P. Wolf. Physics and applications of atmospheric nonlinear optics

- and filamentation, *Opt. Express* **16**, 466-493 (2008)
31. P. Rohwetter, J. Kasparian, K. Stelmaszczyk, Z.Q. Hao, S. Henin, N. Lascoux, W.M. Nakaema, Y. Petit, M. Queisser M, R. Salamé, E. Salmon, L. Wöste, and J.-P. Wolf. Laser-induced water condensation in air, *Nat. Phot.* **4**, 451-456 (2010)
 32. J. Kasparian, R. Ackermann, Y.-B. André, G. Méchain, G. Méjean, B. Prade, P. Rohwetter, E. Salmon, K. Stelmaszczyk, J. Yu, A. Mysyrowicz, R. Sauerbrey, L. Wöste, and J.-P. Wolf. Electric Events Synchronized with Laser Filaments in Thunderclouds, *Opt. Express* **16**, 5757-5763 (2008)